Available online at www.sciencedirect.com
SCIENCE DIRECT®
Journal of Nuclear Materials 324 (2004) 23–32
journal of nuclear materials
www.elsevier.com/locate/jnucmat

Effect of the irradiation–annealing–irradiation cycle on the mechanical properties of pure copper and copper alloy

S.A. Fabritsiev [a,*], A.S. Pokrovsky [b], S.E. Ostrovsky [b]

[a] D.V. Efremov Scientific Research Institute of Electrophysical Apparatus, Doroga na Metallostroy 3, Metallostroy, St. Petersburg 196641, Russia
[b] Scientific Research Institute of Atomic Reactors, Dimitrovgrad 433510, Russia

Received 9 April 2003; accepted 5 September 2003

Abstract

The report presents the results of two irradiation experiments. The first experiment was carried out in the SM-2 reactor with the aim to study the effect of single annealing after irradiation on mechanical properties of pure Cu and GlidCopAl25IG alloy. The aim of the second experiment performed in the RBT-6 reactor was to investigate the effect of the irradiation–annealing–irradiation (IAI) cycle. Pure Cu and GlidCopAl25IG alloy specimens were irradiated in the SM-2 and RBT-6 reactors to $\simeq 10^{-3}$, 10^{-2} and 10^{-1} dpa at $T_{irr} = 80$ °C. The investigations performed revealed that IAI cycles do not cause an accumulation of embrittlement of pure copper and GlidCopAl25IG alloy in the cycles. The experiments lead to the conclusion that the regime of intermediate annealing produces the structure in the material (relatively low density of SFT), sufficiently insensitive to subsequent irradiation (at a low dose level $\simeq 10^{-2}$ dpa).

1. Introduction

Low-temperature radiation embrittlement of pure copper has been investigated since the 1960s. As reported for the first time by Blewitt [1] and Makin [2], irradiation of pure copper at 60 °C to doses of $\simeq 10^{19}$ n/cm^2 involves the emergence of the yield drop on stress–strain curves, hardening and a decrease in uniform and total elongation. Somewhat later the first dose dependences of radiation hardening of pure copper were obtained [2,3]. The effect of annealing at temperatures of 250–650 °C was estimated mainly by changes in electric conductivity and defect structures of irradiated copper specimens [4]. It was shown that annealing at temperatures higher than $0.4T_m$ (where T_m is the melting temperature in Kelvin) can reduce rather effectively the density of radiation defect clusters in copper.

This problem has recently become the topic of practical interest in the framework of activities under the ITER Project. The idea was suggested to use the standard bake-out regime for partial degassing of ITER vacuum vessel components, as well as for partial recovery of the mechanical properties of irradiated materials. As copper alloys of GlidCopAl25 IG, CuCrZr IG type have a very sharp dose dependence of hardening and embrittlement [5,6], attention was focused first of all on the effect of the bake-out regime on these materials. In 2001–2002 the first studies [7,8] demonstrating the efficiency of the bake-out procedure were published. Thus, for example, after irradiation to 0.01–0.3 dpa at 100 °C [7] annealing at 300 °C for 50 h recovered essentially the ductility of OFHC Cu. It was reported in [8] that after irradiation of CuCrZrIG and GlidCopAl25IG alloys at 150 °C to 0.4 dpa annealing at 350 °C for 10 h also recovers the ductility to values close to those for nonirradiated materials. After irradiation at 150 °C to higher doses of ≃2 dpa and annealing at 350 °C for 1 h

* Corresponding author. Tel.: +7-812 464 4463; fax: +7-812 464 4623.
E-mail address: fabrsa@sintez.niiefa.spb.su (S.A. Fabritsiev).

0022-3115/$ - see front matter © 2003 Elsevier B.V. All rights reserved.
doi:10.1016/j.jnucmat.2003.09.004

uniform elongation of alloys was found to recover only partially (to the level of 30–50% of the initial one) [8].

But the vital issue, without solution of which practical justification of the bake-out regime is rather difficult, has remained outside the scope of the above studies. Up to now the data on the effect of subsequent irradiation on the properties of irradiated and then annealed copper alloys have not been obtained. The ITER components, when in operation, will be subjected to the irradiation–annealing–irradiation (IAI) cycle. In principle, this cycle can be repeated many times. Two possible effects of such IAI cycle may be considered. In the first case after irradiation, annealing and subsequent irradiation, the copper alloy may harden and embrittle more than the alloy in the as-irradiated (to the same dose) condition. In this case the real efficiency of bake-out is practically zero, since even though the ductility may recover due to annealing, during the subsequent irradiation the embrittlement rate may increase, and the ductility of the annealed material at the same irradiation dose may have decreased even more than the as-irradiated.

Alternatively the material after post-irradiation annealing may demonstrate weaker embrittlement under subsequent irradiation, and the embrittlement level after the cycle may be less than that for the copper alloy in the as-irradiated (to the same dose) condition.

Experiments were set up to investigate the effect of bake-out on subsequent irradiation hardening and embrittlement of pure Cu and GlidCopAl25 IG copper alloy.

2. Material and experimental procedure

In this study pure Cu (99.987%) with grains 36 μm in size in the annealed condition (550 °C, 2 h) and GlidCopAl25 IG alloy (cross-rolled + annealed) were investigated. Flat specimens of STS type with a gauge length of 10 and 1 mm in thickness were used.

The paper presents the results of two irradiation experiments. The first experiment was carried out in the SM-2 reactor with the aim to study the effect of single annealing. The aim of the second experiment performed in the RBT-6 reactor was to investigate the effect of the IAI cycle. As reported in an earlier publication [9], in the dose range of $\simeq 10^{-3}$ dpa irradiation in SM-2 results in stronger hardening and embrittlement than in RBT-6 due to higher thermal neutron flux, but qualitatively all observed effects in these reactors are similar, and at irradiation doses of $\simeq 10^{-2}$–10^{-1} dpa the coincidence was also quantitative.

Specimens were irradiated in the SM-2 reactor in three irradiation ampoules for 12, 120 and 1253 h yielding displacement damage levels of $\simeq 10^{-3}$, 10^{-2} and 10^{-1} dpa, respectively (Table 1). The fast neutron flux was $\simeq 5\times 10^{17}$ n/m^2 s. The irradiation temperature checked by thermocouples was to (80 ± 5) °C. The specimens were irradiated in helium-filled capsules. The irradiation procedure is described in detail in [9]. After irradiation, some specimens were tested for tension and the rest were annealed in vacuum at 350 °C for 10 h and tensile tested at 80 °C.

Table 1
Irradiation conditions in irradiation facilities of SM-2 and RBT-6 reactors

Reactor, irradiation facility	T_{irr} (°C)	Φt_{fast} ($E > 0.1$ MeV) (n/m^2)	Maximum radiation damage (dpa)	Displacement damage rate (dpa/s)		
SM-2, as irradiated						
SM-2-1	80	1.89×10^{22}	0.0013	3.05×10^{-8}		
SM-2-2	80	1.93×10^{23}	0.0135	3.12×10^{-8}		
SM-2-3	80	2.25×10^{24}	0.1570	3.63×10^{-8}		
RBT-6, as irradiated						
RBT-6-1	75	2.03×10^{22}	0.0014	1.62×10^{-8}		
RBT-6-6	75	1.22×10^{23}	0.0085	1.62×10^{-8}		
RBT-6-7	75	2.2×10^{23}	0.0154	1.68×10^{-8}		
RBT-6-8	75	5.8×10^{23}	0.0407	1.59×10^{-8}		
RBT-6-9	75	1.22×10^{24}	0.0854	1.52×10^{-8}		
RBT-6, IAI cycles	First irradiation (dpa)	First annealing	Second irradiation (dpa)	Second annealing	Third irradiation (dpa)	Total dose on copper after irradiation and annealing (dpa)
RBT-6-2	0.0014	250 °C, 24 h	0.00399	–	–	0.00539
RBT-6-3	0.0014	250 °C, 24 h	0.00399	250 °C, 24 h	0.00465	0.01004
RBT-6-4	0.0014	350 °C, 24 h	0.00456	–	–	0.00596
RBT-6-5	0.0014	350 °C, 24 h	0.00456	350 °C, 24 h	0.0128	0.01876

Five irradiation ampoules were irradiated in the RBT-6 reactor for 24–1560 h yielding accumulation of damage doses in the range of 10^{-3}–10^{-1} dpa. The fast neutron flux was $\simeq 2\times10^{17}$ n/m^2 s. The irradiation regimes and doses for these five ampoules are given in Table 1. The irradiation temperature measured by thermocouples was (75 ± 5) °C.

Four more irradiation ampoules were irradiated in RBT-6 under the same conditions and subjected to intermediate annealing followed by irradiation. Let us use the case of ampoule RBT-6-2 to describe the technology of IAI cycle realization. The ampoule was irradiated in the reactor to a dose of 0.0014 dpa, and then it was withdrawn from the reactor irradiation cell, installed in a special furnace and annealed at 250 °C for 24 h. After annealing the ampoule was again installed in the same reactor cell and subjected to the second irradiation to a dose of 0.004 dpa. After completion of the IAI cycle the ampoule was withdrawn from the reactor, cut, the withdrawn specimens were tensile tested at 80 °C. The irradiation and annealing conditions for all four IAI ampoules are presented in Table 1. The ampoules were filled with helium, thus the specimens were irradiated and annealed in helium.

The specimens were tested in tension (in vacuum) at 80 °C at a strain rate of 1.66×10^{-3} s^{-1}. The microstructure of irradiated specimens was investigated using transmission electron microscopy (TEM). Identical specimens made of the same material were investigated in both irradiation experiments. Three–four specimens per point were tested for SM-2 irradiation and two–three specimens per point were investigated for RBT-6 irradiation.

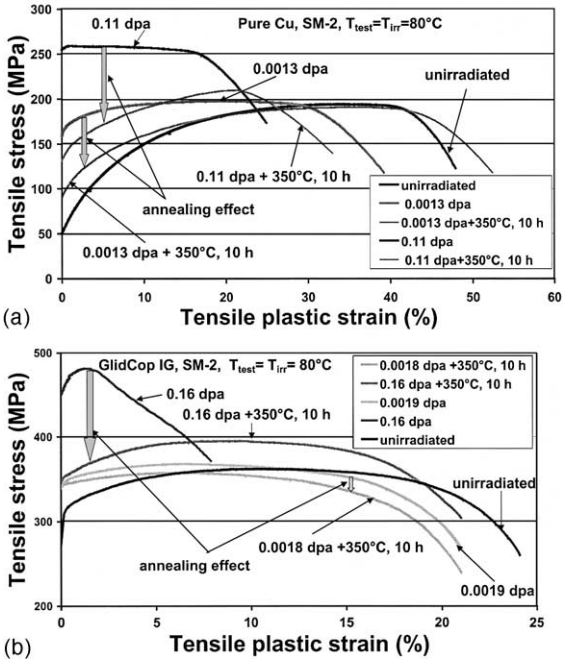

Fig. 1. Effect of post-irradiation annealing at 350 °C for 10 h on the engineering stress–strain curves of (a) pure Cu and (b) GlidCopAl25IG alloy (SM-2 reactor, $T_{test} = T_{irr} = 80$ °C), as-irradiated pure Cu to 0.0013, 0.1577 dpa; irradiated to 0.0013, 0.11 dpa and annealed at 350 °C, 10 h – (a); as irradiated GlidCopAl25IG alloy to 0.0019, 0.078 dpa; irradiated to 0.0018, 0.1559 dpa and annealed at 350 °C, 10 h – (b).

3. Results

3.1. Experiment in SM-2

Fig. 1(a) shows typical engineering stress–strain curves for unirradiated pure Cu, after irradiation to doses of $\simeq10^{-3}$, 10^{-1} dpa, as well as the curves for specimens irradiated to doses of $\simeq10^{-3}$, 10^{-1} dpa and then annealed at 350 °C for 10 h. To make readable Fig. 1, the diagrams of the specimens irradiated to doses of 10^{-2} dpa were not inserted into the figure. On the whole, these diagrams occupy an intermittent position between the diagrams at doses of 10^{-1} and 10^{-3} dpa. As follows from Fig. 1(a), the yield drop appears on the stress–strain curve of pure copper after irradiation to a dose of 10^{-1} dpa. It should be noted that the stress drop was very low (from 3 to 10 MPa), but manifested itself systematically for all specimens irradiated up to doses of 10^{-2}–10^{-1} dpa. The yield drop presence on the stress–strain curves of pure copper for this dose range at $T_{irr} \simeq 50$–100 °C is described in many studies [7,10,11]. After annealing at 350 °C for 10 h the yield drop disappears, the form of the stress–strain curves becomes similar to that for unirradiated material, though the level of yield strength of irradiated pure copper after annealing is still higher by 30–50 MPa than that of the unirradiated one and the uniform elongation is lower by 30–40%.

Fig. 1(b) shows typical engineering stress–strain curves of unirradiated GlidCopAl25IG alloy, irradiated to doses of 10^{-3}, 10^{-1} dpa and irradiated to about the same doses and then annealed at 350 °C for 10 h. As in the case with pure Cu, irradiation to doses of 10^{-2} and 10^{-1} dpa produces the yield drop for GlidCopAl25IG alloy. After annealing at 350 °C for 10 h the yield drop disappears on the stress–strain curves of GlidCopAl25IG. Even though some hardening remains, the curves of annealed specimens are rather similar to the testing curve of unirradiated alloy.

Fig. 2 shows the dose dependence of hardening (change in 0.2% offset yield strength) and uniform elongation of irradiated specimens and specimens annealed after irradiation. The same dependences for GlidCopAl25IG are shown in Fig. 3.

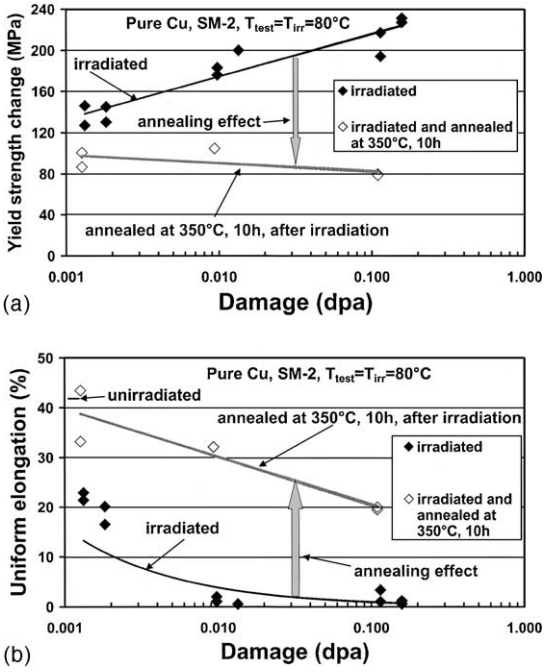

Fig. 2. (a) Change in the 0.2% offset yield strength plotted versus neutron damage for pure Cu: as-irradiated and annealed after irradiation at 350 °C for 10 h; (b) the uniform elongation plotted versus neutron damage for pure Cu: as-irradiated and annealed after irradiation at 350 °C for 10 h, SM-2 reactor, $T_{test} = T_{irr} = 80$ °C.

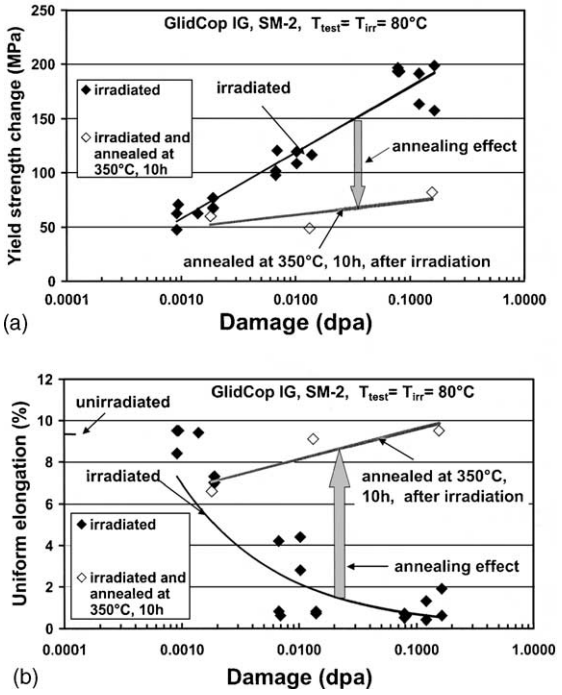

Fig. 3. (a) Change in the 0.2% offset yield strength plotted versus neutron damage for GlidCopAl25IG alloy: as-irradiated and annealed after irradiation at 350 °C for 10 h; (b) the uniform elongation plotted versus neutron damage for GlidCopAl25IG alloy: as-irradiated and annealed after irradiation at 350 °C for 10 h, SM-2 reactor, $T_{test} = T_{irr} = 80$ °C.

On the whole, post-irradiation annealing decreases the radiation hardening level of pure Cu by about 50 MPa at a dose of 10^{-3} dpa and 130 MPa at a dose of 10^{-1} dpa. Uniform elongation of pure Cu is recovered to 70–80% of the initial value at 10^{-3} dpa and amounts to 40% of the initial value at 10^{-1} dpa. Annealing of GlidCopAl25IG alloy specimens irradiated to 10^{-3} dpa does not practically affect hardening and embrittlement. But at doses of $\simeq 10^{-2}$ and 10^{-1} dpa, annealing reduces the radiation hardening level by 40 and 120 MPa, respectively (Fig. 3(a)). Uniform elongation of irradiated specimens after annealing is recovered to the values close to the initial ones (Fig. 3(b)).

On the whole, it is evident that annealing contributes to the deformation processes in irradiated materials, results in a decrease in radiation hardening, disappearance of the yield drop and recovery of the uniform elongation of irradiated specimens to the values close to the initial ones.

As follows from Figs. 2(a) and 3(a), annealing does not completely eliminate radiation hardening of pure copper and GlidCopAl25IG. The residual hardening level after annealing amounts to 50–80 MPa. Therefore, one can expect accumulation of the hardening level in IAI cycles due to summation of the residual hardening levels.

3.2. TEM in SM-2 irradidation

The TEM investigations of the microstructure of pure copper specimens irradiated in SM-2 showed that the structure contains a high density of defect clusters (Fig. 4(a)). The defect density increases with the irradiation dose and at a dose of 10^{-2} dpa attains a value of $\simeq 1 \times 10^{23}$ 1/m^3. The analysis of defect clusters showed that they can be divided into two types, i.e. stacking fault thetraedra (SFT) (Fig. 4(b)) and dislocation loops (DLs) (Fig. 4(a)). Such defect cluster structure is typical of pure copper irradiated at 60–100 °C and was observed in many studies [7,10–12]. In [10–13] it was shown that the SFTs are vacancy clusters and DLs are interstitial clusters. Table 2 presents the results on defect cluster density in irradiated copper obtained by processing the TEM images.

Fig. 4(a) shows, that large loops and dislocation segments are pinned by obstacles. In most cases dislocation segments are decorated by small loops $\simeq 10$ nm in diameter (Fig. 4(a)). Singh et al. [7] observed loop-decorated dislocation lines in OFHC copper irradiated to 10^{-2}–10^{-1} dpa at 80 °C. It is significant that in irradiated specimens no defect-free zones were observed along the grain boundaries.

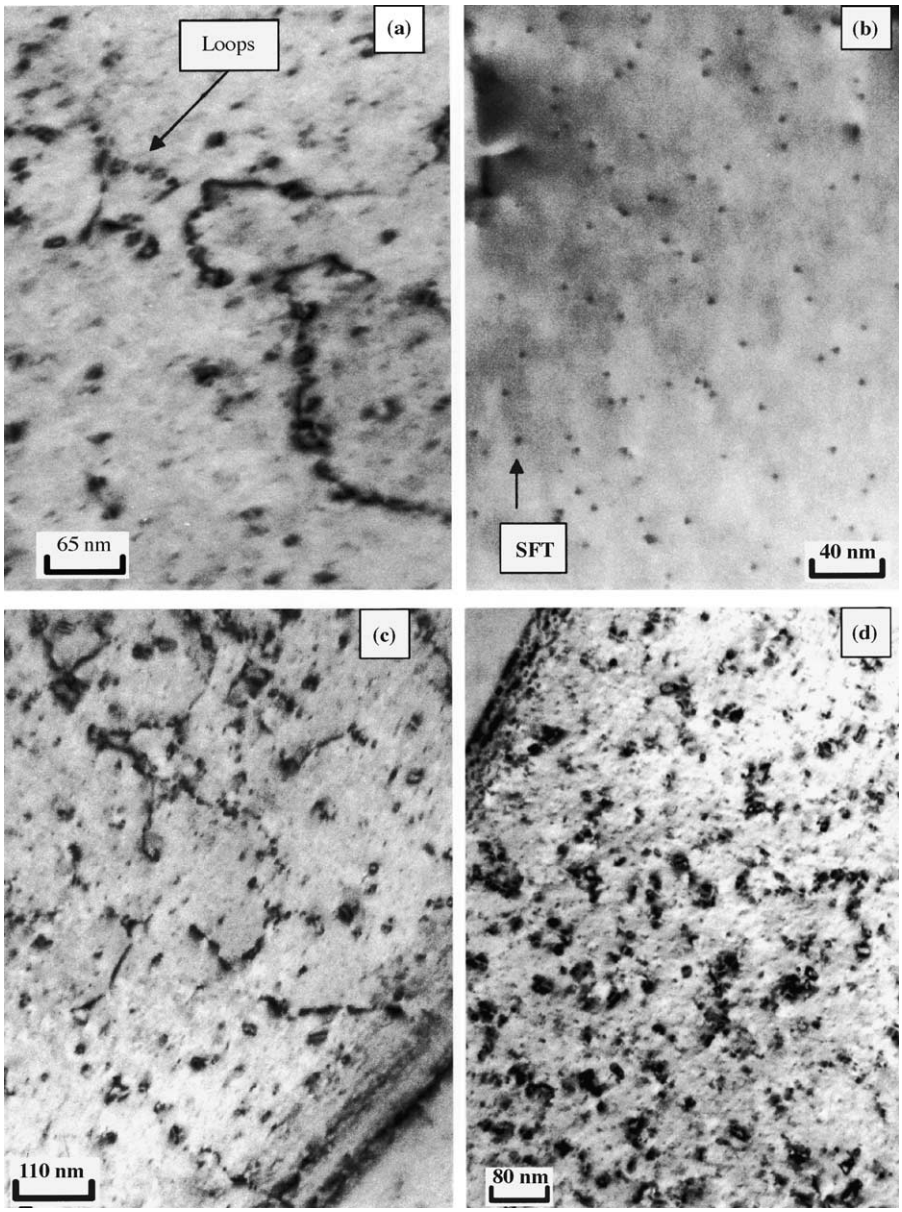

Fig. 4. TEM images of pure Cu: as-irradiated in SM-2 to 0.00978 dpa – (a); annealed at 350 °C, 10 h after irradiation in SM-2 to 0.0094 dpa – (b); as-irradiated in RBT-6 to 0.0154 dpa – (c); after double IAI cycle in RBT-6 (0.0014 dpa + 350 °C, 24 h + 0.00456 dpa + 350 °C, 24 h + 0.0128 dpa) – (d).

Annealing at 350 °C for 10 h results in a change in the structure of irradiated specimens. The DL density is decreased drastically by about an order of magnitude. The size of SFTs is somewhat increased (by about 30%), their density is also low (Table 2 and Fig. 4(b)). Zones free of defect clusters ≃600 nm wide are observed along the grain boundaries. Thus, exposure of irradiated specimens of pure copper at 350 °C for 10 h results in partially annealing of DLs of interstitial type and drop in the SFT density. Thus, moving dislocations are made free from decorating loops. Obviously all these changes in the structure facilitate motion of dislocations in annealed specimens. Correspondingly, hardening is decreased and uniform elongation of annealed specimens is increased, as follows from the stress–strain curves of pure copper (Fig. 1(a)).

Table 2
Defects complex density and size in irradiated pure Cu

Reactor, irradiation facility	IAI regime	Summary damage (dpa)	Density SFT (10^{22} m^{-3})	Mean diameter SFT (nm)	Density DLs (10^{22} m^{-3})	Mean diameter loops (nm)
RBT-6-9	As irradiated	0.0854	12.85	2.27	1.01	10.20
RBT-6-7	As irradiated	0.0154	8.08	2.36	0.43	9.43
RBT-6-2	0.0014 dpa + 250 °C, 24 h + 0.004 dpa	0.0054	6.27	2.20	0.14	9.06
RBT-6-5	0.0014 dpa + 350 °C, 24 h + 0.0046 dpa + 350 °C, 24 h + 0.0129 dpa	0.0188	10.10	2.10	0.33	10.90
SM-2-3	As irradiated	0.1570	12.55	2.25	0.84	10.40
SM-2-2	As irradiated	0.0098	10.50	2.31	0.24	10.56
SM-2-2	Annealed at 350 °C, 10 h, after irradiation	0.0094	1.38	2.62	0.02	9.99

3.3. Experiment in RBT-6

Fig. 5 shows the engineering stress–strain curves of pure copper specimens and GlidCopAl25IG alloy in the unirradiated condition and after irradiation in the dose range of 10^{-3}–10^{-1} dpa in the RBT-6 reactor. As follows from Fig. 5, irradiation at 80 °C results in a monotonous rise in the yield strength and a drop in elongation of both materials with increasing irradiation dose. It is evident that, though the level of yield strength of GlidCopAl25IG alloy is by 280 MPa higher than that of pure Cu, their radiation hardening levels are rather similar. Only in specimens irradiated to a minimum dose of ≃0.0014 dpa the yield drop is lacking. At all higher irradiation doses the yield drop is observed in pure Cu and GlidCopAl25IG in the range of small (≃1%) deformations.

Fig. 6 presents the engineering stress–strain curves for pure copper specimens (Fig. 6(a)) and GlidCopAl25IG (Fig. 6(b)) subjected to the IAI cycle. For pure copper the single IAI cycle causes a considerable radiation hardening, with the uniform elongation of specimens remaining at a rather high level >20%. The yield drop is lacking. The double IAI cycle gives rise to the yield drop on the stress–strain diagrams especially pronounced after irradiation to a maximum dose of 0.0129 dpa.

A comparison between Figs. 5(a) and 6(a) shows that, on the whole, the form of the stress–strain curves of specimens subjected to intermediate annealing is similar to that of specimens as-irradiated to a close dose but the hardening level of the former is somewhat lower.

GlidCopAl25IG alloy (Fig. 6(b)) after the single IAI cycle shows no yield drop. Uniform elongation is ≃4%. Radiation hardening is ≃80 MPa, this being close to the value of $\Delta\sigma_y$ observed in specimens as-irradiated to dose of 0.004 dpa (Fig. 3).

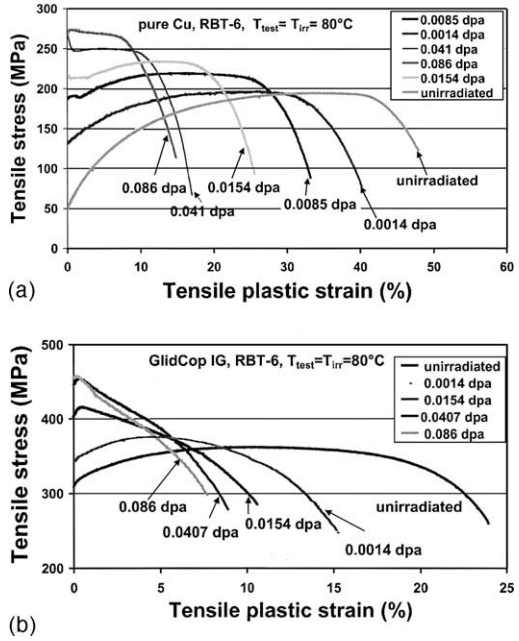

Fig. 5. Effect of neutron irradiation to 0.0014–0.086 dpa on the engineering stress–strain curves of pure Cu – (a); and for GlidCopAl25IG alloy – (b); RBT-6 reactor $T_{test} = T_{irr} = 80$ °C.

The double IAI cycle results in the emergence of the yield drop on the stress–strain curve (Fig. 6(b)). On the whole, the stress–strain curves of such specimens are similar to the curves typical for specimens as-irradiated to a dose of ≃10^{-2} dpa.

One of the remarkable results of the experiments is that intermediate annealing at 250 or 350 °C proved to be practically equivalent in their effect on the properties of pure Cu and GlidCopIG. After the single IAI cycle the stress–strain curves for pure Cu specimens annealed

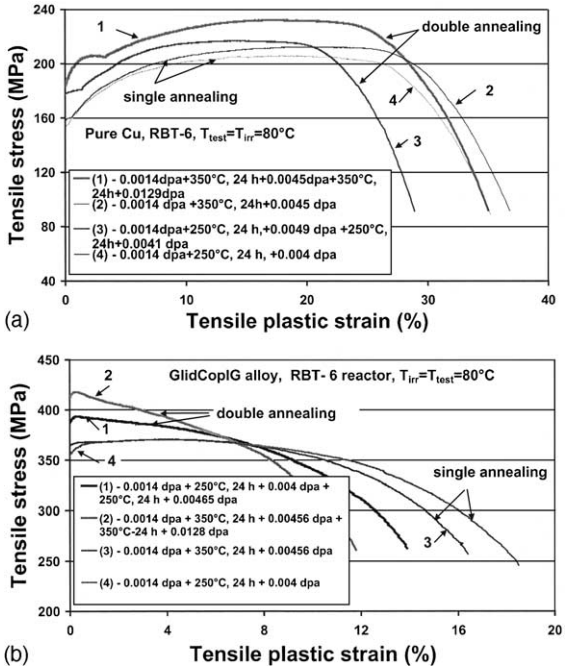

Fig. 6. Effect of IAI cycles on the engineering stress–strain curves of pure Cu – (a); and GlidCopAl25IG alloy – (b); RBT-6 reactor, $T_{test} = T_{irr} = 80$ °C.

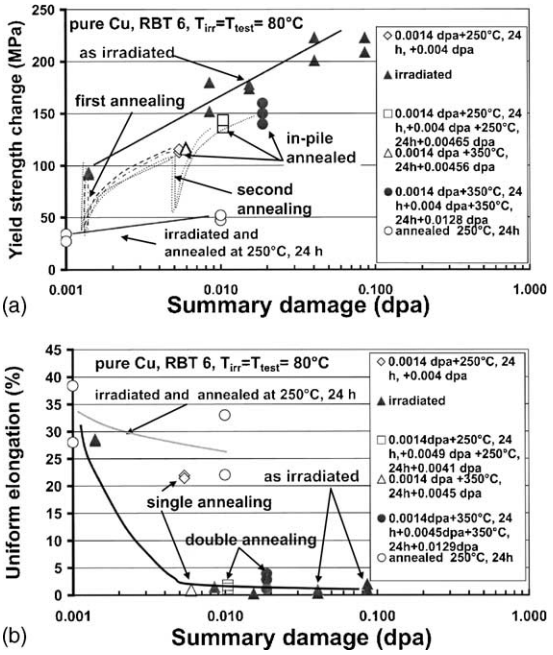

Fig. 7. (a) Change in the 0.2% offset yield strength plotted versus neutron damage for pure Cu: as-irradiated; annealed after irradiation at 250 °C, 24 h; after IAI cycles. Dashed lines demonstrate a possible scheme of change of yield strength during cycles; (b) The uniform elongation plotted versus neutron damage for pure Cu: as-irradiated; annealed after irradiation at 250 °C, 24 h; after IAI cycles. RBT-6 reactor, $T_{test} = T_{irr} = 80$ °C.

at temperatures 250 or 350 °C practically coincide. After the double IAI cycle hardening and embrittlement in specimens annealed at 350 °C are more pronounced than in specimens annealed at 250 °C, but it is related to a higher irradiation dose of specimens annealed at 350 °C.

3.4. Dose dependence in RBT-6 irradiation

Some specimens after irradiation in RBT-6 were subjected to single annealing at 250 °C for 24 h. The rest of specimens were subjected to the IAI cycles by two regimes.

Fig. 7 shows the experimental dependence of radiation hardening on irradiation dose for pure copper specimens irradiated, irradiated and annealed, and subjected to the IAI cycle (reactor RBT-6). Fig. 7 shows also possible scheme of changes in radiation hardening during the IAI cycle. On the whole, the behavior of GlidCopAl25IG alloy in the IAI cycle is similar to that of pure copper (Fig. 8).

3.5. Effect of the IAI cycle on pure copper

3.5.1. Single cycle

Irradiation to 0.0014 dpa increases the yield strength of pure copper by 80 MPa. After intermediate annealing at 250 °C for 24 h $\Delta\sigma_y$ drops to 35 MPa (as follows from the experiments on single annealing). The subsequent second irradiation gives a gain in hardening to about 120 MPa, which is much less than it should be (by hardening dose dependence) for specimens as-irradiated to the same dose (Fig. 7(a)). IAI specimens annealed at 250 °C for 24 h have also a sufficiently high level of uniform elongation of ≃20%. IAI specimens irradiated to slightly higher dose and annealed at 350 °C for 24 h have low uniform elongation (Fig. 7(b)), a slight yield drop is observed (Fig. 6(a) – curve 2).

3.5.2. Double cycle

The double IAI cycle proceeds by the same scheme, i.e. the first IAI cycle, then the second IAI cycle. Annealing reduces hardening of pure copper to ≃50 MPa, and subsequent irradiation causes a gain in hardening by $\Delta\sigma_y \simeq 150$ MPa (Fig. 7(a)). And in this case intermediate annealing reduces hardening to values less than for specimens as-irradiated to the given dose. As this takes place, the specimens have a low uniform elongation associated with instability of deformation at its earlier stages ($\varepsilon < 1\%$) (Fig. 6(a)). Thus it may be concluded that though annealing does not remove hardening completely, subsequent irradiations do not sum up the levels of residual $\Delta\sigma_{y1}$ (irradiated and annealed

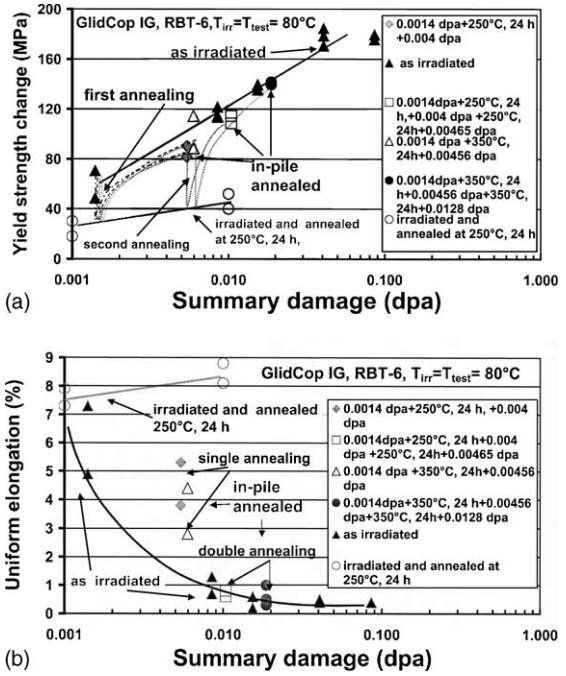

Fig. 8. (a) Change in the 0.2% offset yield strength plotted versus neutron damage for GlidCopAl25IG alloy: as-irradiated; annealed after irradiation at 250 °C, 24 h; after IAI cycles. Dashed lines demonstrate a possible scheme of change of yield strength during cycles; (b) The uniform elongation plotted versus neutron damage for GlidCopAl25IG alloy: as-irradiated; annealed after irradiation at 250 °C, 24 h; after IAI cycles. RBT-6 reactor, $T_{test} = T_{irr} = 80$ °C.

specimen) and $\Delta\sigma_{y2}$ (hardening under subsequent irradiation) but even reduce it. Let us use pure copper to analyze it. In case of an additive addition of hardening the single IAI cycle ($T_{annealing} = 250$ °C) would yield the following:

$$\sum \sigma_{add} = \Delta\sigma_{y1\,irr\,\&\,anneal} + \Delta\sigma_{0.004\,dpa} = 165\ \text{MPa},$$

where $\Delta\sigma_{y1\,irr\,\&\,anneal} = 35$ MPa, $\Delta\sigma_{0.004\,dpa} = 130$ MPa. $\Sigma_{real} = 115$ MPa, that is to say, no damage accumulation occurs in the cycle. The specimens, when under irradiation in the cycle, harden as though the remaining defect component (responsible for hardening of ≃35 MPa) does not at all affect hardening during subsequent irradiation.

3.6. Effect of the IAI cycle on GlidCopIG

As follows from Fig. 8, the single IAI cycle causes hardening of GlidCopAl25IG to the level of about 10 MPa lower than that for as-irradiated alloy. In this case the uniform elongation of the specimens subjected to the IAI cycle remains at a sufficiently high level of ≃3–5%.

After the double IAI cycle, the level of specimen hardening practically coincides with that for as-irradiated specimens. Uniform elongation of such specimens is also low, i.e. ≃1–0.2%. As in the case of pure copper, GlidCopAl25IG specimens annealed at 250 °C demonstrated regularly a lower level of radiation hardening and higher ductility than specimens annealed at 350 °C, though the difference was moderate.

3.7. TEM structure of pure copper specimens irradiated in RBT-6

3.7.1. As-irradiated

As seen from Fig. 4, the TEM structure of pure copper irradiated to 0.0154 dpa in RBT-6 (Fig. 4(c)) is similar, on the whole, to the structure of pure copper irradiated in SM-2 (Fig. 4(a)) to 0.00978 dpa. The structure contains SFTs with a density of $\simeq 10^{23}$ 1/m^3 and DLs with a density of $\simeq 10^{22}$ 1/m^3. The average size of SFTs and loops is ≃2 and ≃10 nm, respectively. As follows from Table 2, at a dose of $\simeq 10^{-2}$ dpa the parameters of the defect cluster structure of the specimens irradiated in RBT-6 and SM-2 are rather close. But there is some difference. At a dose of $\simeq 10^{-2}$ dpa the decoration of dislocations by loops in RBT-6 is pronounced less than in SM-2. The loop density in specimens irradiated in RBT-6 is somewhat higher than in those irradiated in SM-2.

3.7.2. IAI

After the single IAI cycle (250 °C for 24 h) the TEM structure of pure copper is, on the whole, similar to that of as-irradiated pure copper. Rather a high density of SFT is observed in the specimen (Table 2). The microstructure of IAI specimens has distinct qualitative features. First, the dislocation segment density is rather low and they are not decorated with loops. The second to stand out is the absence of large loops (DL) in the IAI specimen. We measured separately the maximum observable size of large loops in all investigated specimens and found that in the IAI specimen this size is half as less again (≃12 nm) than in a specimen as-irradiated to 0.0154 dpa (19 nm). No zones free of defect clusters were observed near the grain boundaries in the IAI specimens.

After the double IAI cycle (350 °C for 24 h) the SFT density in the IAI specimen increases drastically (close to the values observed for a specimen as-irradiated to 0.0154 dpa.). The loop density also increases, but still it is lower than for a specimen as-irradiated to 0.0154 dpa (Fig. 4(d) and Table 2). As in the first case, the size of large DLs is ≃12 nm, which is markedly lower than for as-irradiated specimens. There are no defect-free zones along the grain boundaries. The density of dislocation segments is very low, and they are not decorated with loops.

On the whole, it may be concluded that the IAI cycle, as compared with irradiation to the same dose slightly

increases the density of SFTs and does not practically affect their size, reduces somewhat the density and decreases noticeably the maximum observable size of DLs. Suppression of growth of DLs, their propagation and coalescence to dislocation networks reduces the dislocation density in IAI specimens, the processes of interaction between dislocations and loops (decoration) are suppressed. In IAI specimens, no defect-free zone is observed along the grain boundary.

It may be concluded that the single annealing-produced structure containing a relatively low density of SFT (Fig. 4(b)) suppresses somewhat, when further irradiated, the growth of interstitial loops.

4. Discussion

The investigations performed allow the conclusion that neutron irradiation and annealing and IAI cycle affect substantially the structure and deformation behavior of pure copper. The analysis made reveals two processes in this effect.

The first is the production of the structure during irradiation responsible for pinning of the dislocation sources, stopping of dislocations and decoration of dislocation segments by small loops. All these factors prevent the start of deformation and result in a gain of the yield strength observed in the experiment, as well as in emergence of the yield drop on the stress–strain curves at irradiation doses of >0.008 dpa. Emergence of the yield drop and unstable deformation area in pure copper irradiated at 100 °C to 0.01–0.3 dpa at deformations $\varepsilon \sim 0.01$–0.03 is related, as reported in [7], to the detachment of dislocations from small glisside loops decorating the dislocation lines under irradiation [14].

The effect of radiation defect clusters on the increase of the yield strength of pure copper was investigated in a number of studies [11,12,14], and the formula was proposed to use for the quantitative assessment of $\Delta\sigma_y$ [11]

$$\Delta\sigma_y = \alpha \cdot \mu \cdot m \cdot b(N \cdot d)^{0.5}, \quad (1)$$

where N is the cluster density and d is their diameter, α – the constant describing the complex strength; μ – the elastic modulus; m – the Taylor factor; b – the Burgers vector.

The difficulty in assessing $\Delta\sigma_y$ by formula (1) lies in the fact that there are two types of defects, i.e. SFT and DL, present in irradiated pure copper, which have different α (strength of clusters). But, considering that in irradiated specimens the SFT density is 10 times higher than that of DL, it is possible to neglect the effect of DL, as in [7], and to use in Eq. (1) only the values N and d for SFT. As follows from Table 2, in principle, the contribution of DL to hardening, even with $\alpha_{SFT} = \alpha_{DL}$, can be as high as 30%. Evidently special experiments are needed to estimate the contribution of SFT and DL to hardening.

We have compared our values of SFT density with the curve $\rho_{SFT} \sim \Phi t$ (Φt – fast neutron fluence) constructed in [13] by the results of numerous experiments. In the dose range of 0.001–0.1 dpa two types of behavior are observed, $\rho_{SFT} \sim \Phi t$ and $\rho_{SFT} \simeq (\Phi t)^{0.5}$. The TEM data on the SFT density obtained in our study correspond to $\rho_{SFT} \sim (\Phi t)^{0.5}$. Then it follows from Eq. (1) that $\Delta\sigma \sim (\Phi t)^{0.25}$. As reported in our earlier publication [9], the yield strength of pure copper irradiated in the RBT-6 does vary according to the law $\Delta\sigma \sim (\Phi t)^{0.25}$. Annealing of the specimen irradiated in SM-2 to a dose of $\simeq 10^{-2}$ dpa causes the SFT density to drop by about a factor of 6 (Table 2). A six-fold drop in the SFT density during annealing correlates rather well with a three-fold drop in the hardening level of the specimen irradiated to a dose of 10^{-2} dpa, which was experimentally observed during irradiation. Thus, the experimental values of hardening obtained in our study for irradiated and annealed specimens are rather well described by the mechanisms relating the gain in the yield strength to pinning of dislocations by radiation defect clusters. While using the values of defect cluster density N in irradiated specimens defined by TEM, one can obtain the values of the yield strength gain $\Delta\sigma_y \sim (Nd)^{0.5}$ close to those observed experimentally.

The second effect of neutron irradiation is a drastic drop in the strain hardening coefficient (SHC) of irradiated specimens. As follows from Figs. 1 and 5, neutron irradiation reduces sharply SHC of pure copper. In Ref. [15] we estimated quantitatively the effect of irradiation in SM-2 to doses of 10^{-3}–10^{-1} dpa on SHC of pure copper. A sharp decrease in SHC is observed at irradiation doses of $\geqslant 0.04$ dpa. Annealing recovers the SHC value (Fig. 1).

The IAI cycle causes a moderate increase in the SFT density, a slight drop in the DL density and a decrease in the size of large loops, i.e. it suppresses their growth. Hardening and embrittlement of IAI specimens are somewhat lower than for specimens as-irradiated to this dose. The study of the strain–stress curves of the IAI specimens (Fig. 6) shows that after one IAI cycle both pure copper and GlidCopAl25IG have a relatively low level of radiation hardening and sufficiently large uniform elongation. Therefore, the SFTs remaining in the materials structure after annealing do not enhance radiation hardening during subsequent irradiation. In our opinion, this fact indicates also that DLs play an appreciable role in radiation hardening. No additive summation of materials radiation hardening levels is observed after annealing and subsequent irradiation.

The double IAI cycles result in emergence of the yield drop on the curves. Nevertheless, even after the yield drop, pure copper still retains the capability for deformation, and the deformation values amount to 15–20%

before the loss of stability. The hardening level of specimens after two IAI cycles is somewhat lower than for specimens as irradiated to the same dose. Thus, the IAI cycle, when repeated, does not cause damages to accumulate in the cycles. The structure produced in irradiated specimens after annealing proves to be sufficiently insensitive to subsequent irradiation.

The detailed analysis of the deformation processes and TEM investigations were made mainly for pure copper. At the same time the comparison between the stress–strain curves of pure copper and GlidCopAl25IG alloy (Figs. 1, 5 and 6) shows that qualitatively both these materials behave similarly under irradiation and in the IAI cycle. The difference is only in an essentially higher strength and lesser ductility of GlidCopAl25IG alloy.

5. Conclusions

The investigations performed revealed that the single and double IAI cycles do not cause accumulation of embrittlement of pure copper and GlidCopAl25IG alloy in the cycles. The analysis of the TEM structure of IAI pure copper specimens showed that, as compared with as-irradiated specimens, the growth and coalescence of DLs into networks are suppressed in these specimens. The specimens subjected to the IAI cycle at irradiation doses of >0.0085 dpa demonstrated the yield drop. But after the drop all of them deformed with a sufficiently high SHC, that is to say, the irradiated material still retained the capability for hardening. One should take into account that all conclusions are based on the results obtained in the dose range of relatively low irradiation doses of $\simeq 10^{-2}$ dpa and their extrapolation is possible only after experiments at higher irradiation doses.

The experiments lead to the conclusion that the bake-out regime of intermediate annealing produces a structure in the material (relatively low density of SFT), sufficiently insensitive to subsequent irradiation. The conclusion is made that the bake-out regime holds promises for ITER applications as a technological procedure reducing the embrittlement level of alloys.

Acknowledgement

The authors would like to thank Dr V. Barabash for helpful discussions of the ideas of the experiment.

References

[1] T. Blewitt, R. Coltman, J. Redman, in: Proceedings of the International Conference Dislocation and Mechanical Properties of Crystals, Lake Placid, USA, 6–8 September 1956, New York, 1957, p. 125.
[2] M.J. Makin, in: W.F. Sheely (Ed.), Radiation Effects, Gordon and Breach Science Publishers, New York, 1967, p. 627.
[3] I.A. El-Shanshoury, J. Nucl. Mater. 45 (1972/1973) 245.
[4] T. Blewitt, R. Coltman, J. Appl. Phys. 28 (1957) 639.
[5] A.S. Pokrovsky, S.A. Fabritsiev, D.J. Edwards, S.J. Zinkle, A.F. Rowcliffe, J. Nucl. Mater. 283–287 (2000) 404.
[6] D.J. Edwards, B.N. Singh, Q. Xu, P. Toft, J. Nucl. Mater. 307–311 (2002) 439.
[7] B.N. Singh, D.J. Edwards, P. Toft, J. Nucl. Mater. 299 (2001) 205.
[8] S.A. Fabritsiev, A.S. Pokrovsky, J. Nucl. Mater. 307–311 (2002) 431.
[9] S.A. Fabritsiev, A.S. Pokrovsky, J. Nucl. Mater. 306 (2002) 78.
[10] B.N. Singh, A. Horsewell, P. Toft, D.J. Edwards, J. Nucl. Mater. 224 (1995) 131.
[11] B.N. Singh, D.J. Edwards, P. Toft, J. Nucl. Mater. 238 (1996) 244.
[12] S.J. Zinkle, J. Nucl. Mater. 150 (1987) 140.
[13] B.N. Singh, S.J. Zinkle, J. Nucl. Mater. 206 (1993) 212.
[14] B.N. Singh, A. Horsewell, P. Toft, D.J. Edwards, J. Nucl. Mater. 224 (1995) 131.
[15] S.A. Fabritsiev, A.S. Pokrovsky, Fus. Eng. Design 65 (2003) 545.